

Somatostatin receptor subtype 2 sensitizes human pancreatic cancer cells to death ligand-induced apoptosis

Julie Guillermet*, Nathalie Saint-Laurent*, Philippe Rochaix†, Olivier Cuvillier‡, Thierry Levade‡, Andrew V. Schally§, Lucien Pradayrol*, Louis Buscail*, Christiane Susini*, and Corinne Bousquet*¶

*Institut National de la Santé et de la Recherche Médicale (INSERM) U531, †Institut National de la Santé et de la Recherche Médicale (INSERM) U466, Institut Federatif de Recherche (IFR) 31, Centre Hospitalier Universitaire (CHU) Rangueil, and ‡Laboratoire d'Anatomopathologie, Institut Claudius Regaud, 31403 Toulouse, France; and §Veterans Affairs Medical Center and Tulane University School of Medicine, New Orleans, LA 70146

Contributed by Andrew V. Schally, November 6, 2002

Somatostatin receptor subtype 2 (*sst2*) gene expression is lost in 90% of human pancreatic adenocarcinomas. We previously demonstrated that stable *sst2* transfection of human pancreatic BxPC-3 cells, which do not endogenously express *sst2*, inhibits cell proliferation, tumorigenicity, and metastasis. These *sst2* effects occur as a consequence of an autocrine *sst2*-dependent loop, whereby *sst2* induces expression of its own ligand, somatostatin. Here we investigated whether *sst2* induces apoptosis in *sst2*-transfected BxPC-3 cells. Expression of *sst2* induced a 4.4- ± 0.05-fold stimulation of apoptosis in BxPC-3 through the activation of tyrosine phosphatase SHP-1. *sst2* also sensitized these cells to apoptosis induced by tumor necrosis factor α (TNF α), enhancing it 4.1- ± 1.5-fold. Apoptosis in BxPC-3 cells mediated by TNF-related apoptosis-inducing ligand (TRAIL) and CD95L was likewise increased 2.3- ± 0.5-fold and 7.4- ± 2.5-fold, respectively. *sst2*-dependent activation and cell sensitization to death ligand-induced apoptosis involved activation of the executioner caspases, key factors in both death ligand- or mitochondria-mediated apoptosis. *sst2* affected both pathways: first, by up-regulating expression of TRAIL and TNF α receptors, DR4 and TNFR1, respectively, and sensitizing the cells to death ligand-induced initiator caspase-8 activation, and, second, by down-regulating expression of the antiapoptotic mitochondrial Bcl-2 protein. These results are of interest for the clinical management of chemoresistant pancreatic adenocarcinoma by using a combined gene therapy based on the cotransfer of genes for both the *sst2* and a nontoxic death ligand.

Pancreatic carcinoma is the fifth leading cause of cancer-related deaths in Western countries, with an overall 1-year survival rate of \approx 12%. Most patients are not candidates for surgery because by the time the diagnosis is established, the disease has already progressed. Conventional nonsurgical treatments are generally ineffective because pancreatic cancer cells are resistant to cytotoxic agents and radiation (1), and human pancreatic adenocarcinomas fail to respond to conventional chemotherapy (2). Therefore, a better understanding of the molecular changes that occur in pancreatic cancer would be of great interest for the development of more effective therapeutic approaches for this incurable disease.

Somatostatin is a ubiquitous neuropeptide mainly expressed in the central and peripheral nervous system, and in the gastrointestinal tract, including the pancreas. Somatostatin inhibits multiple functions, including exocrine and endocrine secretions, inflammation, and angiogenesis, as well as cell proliferation and tumorigenesis, as shown in normal or tumoral cell models (3–5). Somatostatin receptor subtype 2 (*sst2*) belongs to the G protein-coupled receptor family for somatostatin, which comprises five subtypes, *sst1*–*5*. We previously demonstrated selective loss of the *sst2* protein in 90% of pancreatic adenocarcinomas and derived cell lines (6). Reexpression of *sst2* in the human pancreatic cancer BxPC-3 cells, which do not endogenously express the *sst2* protein, results in an *sst2*-dependent inhibition of cell

proliferation and tumorigenesis, observed *in vitro*, and also *in vivo* in athymic mice injected s.c. with *sst2*-transfected BxPC-3 cells (7, 8). Molecular mechanisms involved in the antiproliferative and antitumorigenic action of *sst2* depend on an *sst2*-dependent induction of somatostatin expression, which in turn constitutively activates the *sst2* receptor. In addition to the BxPC-3 cell model, this *sst2*-somatostatin autocrine loop was also demonstrated in human Capan-1 or hamster PC1-0 pancreatic cancer cells, and in murine fibroblastic NIH 3T3 cells (9, 10). In the athymic mouse model, *sst2*-dependent tumor growth inhibition was associated with decreased Ki67 proliferative index and an induction of apoptosis in the *sst2*-expressing tumors (8).

Impaired apoptosis has been implicated in the development of many human diseases, including cancer (11). Two main signaling pathways initiate the apoptotic program in mammalian cells (12). The cell-extrinsic pathway triggers apoptosis in response to activation by their respective ligand of the tumor necrosis factor (TNF) family of death receptors, including TNF-RI for TNF α , Fas or CD95 for FasL, and death receptor 4 (DR4) or 5 (DR5) for TNF-related apoptosis-inducing ligand (TRAIL). On the other hand, the cell-intrinsic pathway triggers apoptosis in response to DNA damage, loss of survival factors, or other types of cell distress. Both pathways involve the activation of cysteine proteases called caspases, which are constitutively expressed in the cytosol as proenzymes, and are activated to mature proteases by cleavage. Activation of the caspases is responsible for the cell damage observed during apoptosis (12).

Tumor cell death induced by chemotherapy and radiotherapy is mediated by the activation of apoptosis. However, most pancreatic adenocarcinoma cell lines are resistant to death receptor- and mitochondria-initiated apoptosis (2, 13).

In this work, we investigated whether *sst2* induces apoptosis in *sst2*-transfected BxPC-3 cells. In addition, we explored whether these cells, which normally have a low sensitivity to apoptosis induced by death ligands, can be sensitized by transfection of *sst2* to induce cell death mediated by TNF α , TRAIL, or antibody to CD95.

Materials and Methods

Cell Culture. Human pancreatic cancer BxPC-3 cells were transfected with either the human 1.35-kbp *sst2* cDNA or the mock vector (7, 9). Stable BxPC-3 transfectants were selected by using 0.4 mg/ml geneticin and cultured in DMEM supplemented with

Abbreviations: CK18, cytokeratin 18; DR, death receptor; TNF, tumor necrosis factor; TRAIL, TNF-related apoptosis-inducing ligand; *sst1*–*5*, somatostatin receptor subtypes 1–5; TNFR1, TNF α receptor; PARP, poly(ADP-ribose) polymerase; MTT, 3-(4,5-dimethylthiazol-2-yl)-2,5-diphenyl tetrazolium bromide; COXII, cytochrome oxidase subunit II.

¶To whom correspondence should be addressed at: INSERM U531, IFR 31, CHU Rangueil, Bât L3, 1 Avenue Jean Poulhès, 31403 Toulouse, France. E-mail: corinne.bousquet@toulouse.inserm.fr.

10% FCS, 2.5 $\mu\text{g/ml}$ Fungizone, 2 mM L-glutamine, and 5 units/ml streptomycin/penicillin (Invitrogen).

Cells were treated with 10 ng/ml TNF α (Preprotech, Le Perray en Yvelines, France), 10 $\mu\text{g/ml}$ cycloheximide (Sigma), 100 ng/ml TRAIL (Preprotech), or 100 ng/ml anti-CD95 Ab (Immunotech, Marseille, France). All TNF α treatments were performed in the presence of 10 $\mu\text{g/ml}$ cycloheximide. The Bcl-2 inhibitor HA14-1 (Alexis, Paris) was used at 50 μM .

Caspase-Cleaved Cytokeratin 18 (CK18) Immunocytochemistry. Cells were grown (10^5 cells per ml) and then starved for 48 h in the presence of Asp-Glu-Val-Asp-aldehyde (DEVD-CHO) or its absence (control), or treated for 12 h with TNF α + cycloheximide, TRAIL, or anti-CD95 Ab. Control cells were not treated with the death ligands. Cells were fixed in PreservCyt (CYTYC, Marlborough, MA) and spread on slides with a cytospin. The cleaved CK18 was immunodetected by using DAKO reagents and the anti-cleaved CK18 M30 cytodeath primary antibody (Roche Molecular Biochemicals) was used according to the manufacturer's instructions. Negative control slides were prepared by replacing the primary antibody with PBS.

Image Processing. Cleaved CK18 immunocytochemistry staining was visualized by using an optical microscope coupled to a Visiolab 2000 image analyzer (Biocom, Paris). The percentage of labeled cells was evaluated on the basis of >1,000 cells in 15–20 successive high-power ($\times 40$) fields.

Cell Viability Assay. Cells were grown (10^4 cells per well) and then treated for 24 h with TNF α + cycloheximide, TRAIL, or anti-CD95 Ab, or in the absence of the death ligands. Mitochondrial viability was measured by using the 3-(4,5-dimethylthiazol-2-yl)-2,5-diphenyl tetrazolium bromide (MTT; Sigma) colorimetric assay (14).

Executioner Caspase Activity Assay. Cells were grown (10^5 cells per ml), starved for 15 h, and treated for 4 h with TNF α + cycloheximide, TRAIL, or anti-CD95 Ab. Control cells were not treated with the death ligands. The executioner caspase activity assay was performed by using the Quantipak kit (Biomol, Perray en Yvelines, France) on 50- μg cytosolic extracts with 200 μM of the specific caspase-3 chromogenic substrate Z-Asp-Glu-Val-Asp-*para*-nitroaniline (DEVD-pNA), according to the manufacturer's instructions. Samples containing no cell extracts were used as negative controls. Inhibition of the executioner caspase activity was carried out with the specific inhibitor DEVD-CHO.

Preparation of Whole-Cell Extracts and Western Blot Analysis. To generate whole-cell extracts, cells were lysed in 50 mM Tris-HCl, pH 7.4/100 mM KCl/10% glycerol/1 mM EDTA/1% Triton X-100/1 mM DTT/protease inhibitors (Roche). After two freeze-thaw cycles, samples were centrifuged at $10,000 \times g$ (for 5 min at 4°C). Soluble proteins were resolved by SDS/PAGE and transferred to a nitrocellulose membrane (Biotrace NT, 0.45 μm , Gelman). After probing with a specific primary antibody and a horseradish peroxidase-conjugated secondary antibody, the protein bands were detected by enhanced chemiluminescence (Pierce). Primary antibodies used were as follows: anti-caspase 3, anti-human TNF α receptor (TNFRI), anti-DR5, anti-Bcl-X_L, and anti-histone (Santa Cruz Biotechnology), anti-SHP-1 (Transduction Laboratories, Lexington, KY), anti-DR4, anti-Bcl-2, anti-Bak, and anti-Bax (Upstate Biotechnology, Souffelweyersheim, France), anti-Mcl-1 (PharMingen), anti-CD95 (Becton Dickinson), anti-poly(ADP-ribose) polymerase (PARP; Roche), and anti-caspase 8 [a kind gift of G. Cohen, University of Leicester, Leicester, U.K. (15)].

Transient Transfection of SHP-1 and C453S-SHP-1 cDNA. Mock- and sst2-transfected cells were transfected with 5 μg of pcDNA3.1/SHP-1, or pcDNA3.1/C453S-SHP-1, or pcDNA3.1 vector (Invitrogen), with 25 μl of polyethylenimine (Exgen 500 transfection reagent, Upstate Biotechnology). After 24 h of growth in 10% FCS and 15 h without FCS, cells were used for an executioner caspase activity assay.

mRNA Quantification by Real-Time Quantitative PCR. Total RNA was extracted with RNable (Eurobio, Paris) according to the manufacturer's instructions. After a DNase treatment, total RNA was reverse transcribed by using random hexamer primers. Resulting cDNAs were used in a real-time quantitative PCR on the Abiprism 5800 using Sybr green as a dye (Applied Biosystems) and specific primers (MWG Biotech, Ebersberg, Germany) for 18S rRNA (sense 5'-AAACGGCTACCACATCCAAG-3', antisense 5'-CCTCCAATGGATCCTCGTTA-3'), TNFRI (sense 5'-TGCTTCAATTGCAGCCTCTG-3', antisense 5'-TCGTGCACTCCAGGCTTTT-3'), DR4 (sense 5'-CTGCTG-CAGGTGCTACCTAGC-3', antisense 5'-CTGTGCACCGGT-TACAGGC-3'), DR5 (sense 5'-GACCTCCTTTTCTG-CTTGCG-3', antisense 5'-GCACTTCCGGCACATCTCA-3'), and CD95 (sense 5'-ATGAACCAGACTGCGTGCC-3', antisense 5'-GTATTCTGGGTCCGGGTGC-3'). PCR efficiencies were measured by preparing a standard curve for each primer pair (efficiency >85%). Target gene expression was normalized by using the 18S rRNA expression as an internal control. Samples incubated without reverse transcriptase were used as negative template controls.

Preparation of Mitochondrial and Cytosolic Extracts. Mitochondrial and cytoplasmic preparations were carried out as described (14). The cytosolic fraction containing cytochrome *c* was first immunoprecipitated with an anti-cytochrome *c* antibody (Becton Dickinson) and the resulting immunoprecipitates were used in a Western blot with another anti-cytochrome *c* antibody (PharMingen). Cytosolic and mitochondrial fractions of the cytochrome oxidase subunit II (COXII) and the cytosolic fraction of histone were assessed by Western blots with an anti-COXII (Molecular Probes) or an anti-histone (Santa Cruz Biotechnology) antibody, respectively.

Statistical Analysis. Statistical analysis was performed by unpaired *t* test. All values are mean \pm SEM.

Results

sst2 Induces an Executioner Caspase-Dependent Apoptosis. We previously demonstrated in BxPC-3 cells stably transfected with the human sst2 cDNA (BxPC-3/sst2), that the autocrine sst2-somatostatin loop results in sst2-mediated inhibition of cell proliferation and tumorigenesis (7). We therefore investigated whether sst2 induces apoptosis in this model. Apoptosis was quantified by using immunocytochemistry of the cleaved form of the human CK18. sst2 expression induced apoptosis 4.4 ± 0.5 -fold in BxPC-3/sst2 after 48-h cell starvation, as compared with mock-transfected cells (Fig. 1a). Treatment of cells with the specific executioner caspase inhibitor DEVD-CHO abrogated sst2-mediated apoptosis, and it reverted apoptosis levels in BxPC-3/sst2 to those observed in the mock-transfected cells (Fig. 1a). These results demonstrated that transfection of sst2 in BxPC-3 cells stimulates an executioner caspase-dependent apoptosis. By using a cell viability assay (MTT), we showed that sst2 decreased cell viability in BxPC-3/sst2 to $64 \pm 1.4\%$ of BxPC-3/mock cells (100%; $P < 0.01$; Fig. 1b).

sst2 Sensitizes BxPC-3 Cells to Death Ligand-Induced Apoptosis. Because pancreatic cancer cells respond poorly to death ligand-induced apoptosis (13), we investigated whether sst2 sensitizes

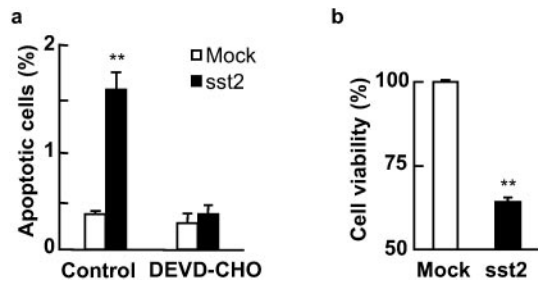


Fig. 1. Quantification of cell death in BxPC-3 cells expressing or not expressing sst2. (a) Mock- and sst2-transfected BxPC-3 were grown and starved for 48 h in the presence or absence (control) of 10 μ M DEVD-CHO. Apoptotic cells were detected by immunocytochemistry of cleaved CK18. Results are expressed as mean \pm SEM ($n = 3$). (b) MTT assay. Mock- and sst2-transfected BxPC-3 cells were grown (10^4 cells per well) and starved for 48 h. Data points represent the mean \pm SEM ($n = 3$) and are expressed as the percentage of the cell viability observed in mock-transfected cells. *, $P < 0.05$; **, $P < 0.01$ for sst2- vs. mock-transfected cells.

these cells to TNF α -, TRAIL-, or CD95 Ab-induced cell death. Apoptosis was increased by a 12-h cell stimulation with TNF α (18.8- \pm 2-fold), TRAIL (8.4- \pm 2.7-fold), or, to a lesser extent, CD95 Ab (3.9- \pm 0.5-fold) in BxPC-3/mock cells, as compared with untreated controls (not shown). sst2 strongly enhanced apoptosis induced by TNF α (4.1- \pm 1.5-fold), TRAIL (2.3- \pm 0.5-fold) or CD95 Ab (7.4- \pm 2.5-fold) in BxPC-3/sst2 cells, as compared with the mock-transfected cells (Fig. 2a). To confirm these results, the effect of sst2 on cell viability, as measured in an MTT assay, was assessed in mock- and sst2-transfected

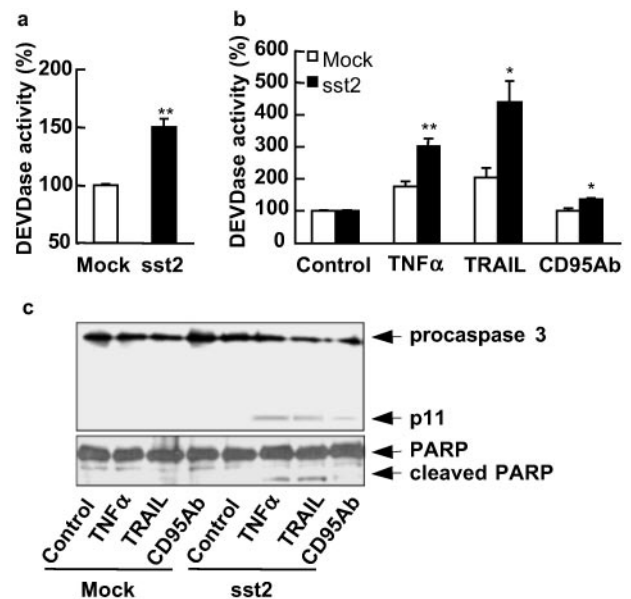


Fig. 3. Basal and death ligand-induced executioner caspase activity in BxPC-3 cells expressing or not expressing sst2. (a-c) Mock- and sst2-transfected BxPC-3 cells were grown and starved for 15 h (a), and treated for 4 h with TNF α + cycloheximide, TRAIL, or anti-CD95 Ab, except for the control (b and c). (a and b) Executioner caspase activity assay. Results are presented as the percentage of executioner caspase activity measured in mock-transfected cells (a) or in untreated control cells (b) and expressed as mean \pm SEM ($n = 5$). *, $P < 0.05$; **, $P < 0.01$ for sst2- vs. mock-transfected cells. (c) Immunoblots using anti-caspase 3 (Upper) and anti-PARP (Lower) antibodies. The expression of histone was used as an internal loading control (not shown; $n = 3$).

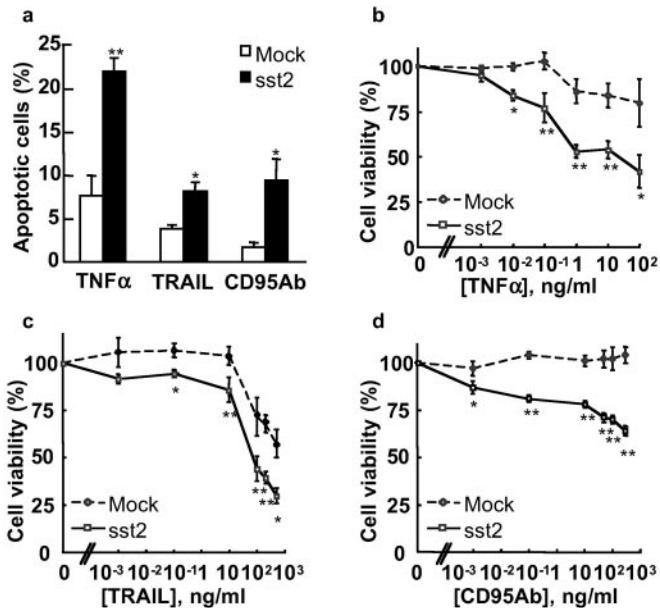


Fig. 2. Quantification of death ligand-induced cell death in BxPC-3 cells expressing or not expressing sst2. (a) Mock- and sst2-transfected BxPC-3 cells were grown and treated for 12 h with TNF α + cycloheximide, TRAIL, or anti-CD95 Ab. Apoptotic cells were identified by using the same technique as in Fig. 1a. Results are expressed as mean \pm SEM ($n = 3$). (b-d) MTT assay. Mock- and sst2-transfected BxPC-3 cells were grown and treated for 24 h with increasing doses of TNF α (0–100 ng/ml) together with a constant dose of 10 μ g/ml cycloheximide (b), TRAIL (0–300 ng/ml) (c), or anti-CD95 Ab (0–500 ng/ml). (d) Data points represent the mean \pm SEM ($n = 3$) and are expressed as the percentage of the cell viability observed either in cycloheximide-treated cells for TNF α treatment or in untreated cells for the other treatments. *, $P < 0.05$; **, $P < 0.01$ for sst2- vs. mock-transfected cells.

BxPC-3 stimulated with increasing doses of TNF α (0–100 ng/ml), TRAIL (0–500 ng/ml), or CD95 Ab (0–300 ng/ml; Fig. 2 b–d). The viability of untreated BxPC-3/sst2 cells was 59 \pm 3% ($P < 0.01$) of untreated BxPC-3/mock cells, and 57 \pm 1.5% ($P < 0.01$) in the presence of 10 μ g/ml cycloheximide. While the death ligands did not appreciably decrease the viability of BxPC-3/mock cells, cell viability in BxPC-3/sst2 was dose-dependently reduced by treatment with TNF α , TRAIL, or CD95 Ab. Calculated K_d for BxPC-3/mock and BxPC-3/sst2 cells, respectively, are 290 and 0.18 ng/ml for TNF α , 250 and 32 ng/ml for TRAIL, and 0.07 ng/ml for CD95 Ab in BxPC-3/sst2 (not detectable in BxPC-3/mock cells).

sst2 Both Stimulates and Sensitizes Cells to a Death Ligand-Induced Executioner Caspase Activity. To investigate whether sst2-induced apoptosis and cell sensitization to death ligand-induced apoptosis correlate with sst2-mediated stimulation of an executioner caspase activity, we measured, in a quantitative assay using DEVD-pNA as a substrate, the DEVDase executioner caspase activity in mock- and sst2-transfected BxPC-3 cells (Fig. 3a and b). sst2 expression resulted in enhanced ($P < 0.01$) DEVDase activity in BxPC-3/sst2 cells (1.5- \pm 0.07-fold of BxPC-3 mock cells; Fig. 3a). DEVDase activity was stimulated by 4-h treatment with TNF α (1.8- \pm 0.2-fold), or TRAIL (2.1- \pm 0.3-fold) in BxPC-3/mock cells, whereas CD95 Ab treatment was not very effective on BxPC-3/mock cells, the stimulation being only 1.1- \pm 0.05-fold (Fig. 3b). Most importantly, sst2 enhanced DEVDase activity induced by 4-h treatment with TNF α (1.7- \pm 0.1-fold), TRAIL (2- \pm 0.1-fold), or CD95 Ab (1.4- \pm 0.06-fold) in BxPC-3/sst2 cells, as compared with BxPC-3/mock cells (Fig. 3b).

These results were further confirmed by Western blots using either an anti-caspase 3 antibody, which recognizes both the procaspase and the cleaved active caspase 3 p11 (Fig. 3c

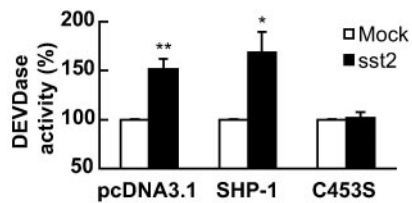


Fig. 4. Effect of transient transfection of BxPC-3 cells with a catalytically inactive SHP-1 (SHP-1/C453S) cDNA on *sst2*-induced activation of the executioner caspase activity. Mock- and *sst2*-transfected BxPC-3 cells were grown and transiently transfected with cDNA encoding wild-type SHP-1 or the catalytically inactive SHP-1 (C453S), or with the empty plasmid (pcDNA3.1). Results are presented as the percentage of the executioner caspase activity measured in mock-transfected cells and expressed as mean \pm SEM ($n = 5$). *, $P < 0.05$; **, $P < 0.01$ for *sst2*- vs. mock-transfected cells.

Upper), or an anti-PARP (a caspase substrate) antibody, which similarly recognizes the full and the cleaved form of PARP (Fig. 3c Lower). Neither the p11 cleaved active subunit of the caspase 3 nor the cleaved form of PARP was observed in untreated mock- and *sst2*-transfected BxPC-3 cells (Fig. 3c). In contrast, procaspase 3 and PARP were cleaved after 4-h treatment with the death ligands in the BxPC-3/*sst2* cells, but not in mock-transfected cells. These results indicate that *sst2* both stimulates and sensitizes the cells to death ligand-induced apoptosis and executioner caspase activity.

SHP-1 Is a Critical Effector for *sst2*-Induced Executioner Caspase Activation. We previously reported that the tyrosine phosphatase SHP-1, containing an SH2 domain, is a critical *sst2*-coupled signaling molecule (16). To investigate molecular mechanisms involved in the *sst2*-induced executioner caspase activation, we explored whether SHP-1 is implicated in *sst2* action. BxPC-3 *sst2*-transfectants were transiently transfected with cDNA encoding wild-type SHP-1 or the catalytically inactive C453S SHP-1 form, or with the empty pcDNA3.1 vector. In pcDNA3.1-transfected BxPC-3/*sst2* cells, *sst2* stimulated DEVDase activity 1.5 ± 0.08 -fold, as compared with BxPC-3/mock cells (Fig. 4). Although similar increases in DEVDase activities were observed in both wild-type SHP-1- and pcDNA3.1-transfected BxPC-3/*sst2* cells, transfection of the C453S form of SHP-1 abrogated *sst2*-induced DEVDase activity in BxPC-3/*sst2* cells to levels observed in BxPC-3/mock cells. As a transfection control, similar levels of both the wild-type and mutated C453S form of SHP-1 expression were observed in a Western blot (not shown). These results demonstrate a critical role for SHP-1 in *sst2*-induced executioner caspase activation.

***sst2* Acts on the Death Ligand-Triggered Signaling Pathway.** Death ligand-triggered apoptosis involves, as an upstream event, the activation of the initiator caspase 8. To study the molecular mechanisms implicated in *sst2*-mediated cell-sensitization to death ligand-induced apoptosis, we investigated whether *sst2* sensitizes cells to death ligand-induced caspase 8 activity by Western blot analysis using an antibody that recognizes both the procaspase and the cleaved active subunits of caspase 8 (p41–43 and p16; Fig. 5a). Strikingly, basal and death ligand-induced cleavage of the caspase 8 (p16 subunit) was increased in BxPC-3/*sst2* cells.

We then explored whether *sst2* might up-regulate death ligand receptor mRNA and/or protein. First, we measured receptor mRNA expression, TNFRI for TNF α , DR4 and DR5 for TRAIL, and Fas (CD95) for FasL, in 24-h-starved BxPC-3/mock or BxPC-3/*sst2* cells, using real-time quantitative RT-PCR analysis (Fig. 5b). TNFRI, DR5, or CD95 mRNA expression was not affected by *sst2* transfection, but DR4 mRNA expression was

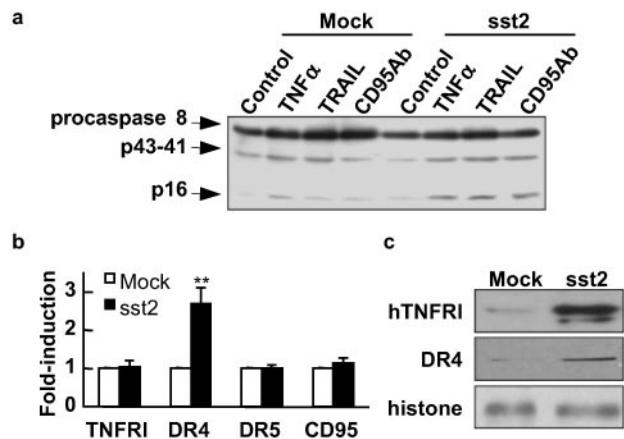


Fig. 5. Effect of *sst2* transfection on the death ligand-triggered signaling pathway in BxPC-3 cells. (a) Mock- and *sst2*-transfected BxPC-3 cells were grown (10^5 cells per ml) and starved for 15 h, and treated (except for control) for 4 h with TNF α + cycloheximide, TRAIL, or anti-CD95 Ab. For immunoblotting, an anti-caspase 8 antibody was used ($n = 3$). (b and c) Mock- and *sst2*-transfected BxPC-3 cells were grown (10^5 cells per ml) and starved for 24 h. (b) Real-time quantitative RT-PCR was performed to determine changes in the expression of TNFRI, DR4, DR5, and CD95 mRNA, respectively. Results are expressed as fold induction over mRNA expression observed in mock-transfected BxPC-3 cells and represent the mean \pm SEM ($n = 4$). *, $P < 0.05$; **, $P < 0.01$ for *sst2*- vs. mock-transfected cells. (c) Immunoblots using the anti-DR4 and anti-TNFRI antibodies on whole-cell protein extracts of BxPC-3. The expression of histone was used as an internal loading control ($n = 3$).

increased (2.7 ± 0.4 -fold; $P < 0.01$) in BxPC-3/*sst2* cells. In addition, a Western blot assay using an anti-DR4 antibody showed *sst2*-dependent up-regulation of DR4 protein (5 ± 1.1 -fold; $P < 0.05$) in BxPC-3/*sst2* (Fig. 5c Middle). Similarly, expression of the TNFRI protein was dramatically up-regulated in BxPC-3/*sst2* (4.9 ± 1.8 -fold; $P < 0.05$) (Fig. 5c Top). In contrast, and in accord with the real-time quantitative RT-PCR results, we did not detect *sst2*-dependent regulation of DR5 or CD95 protein expression (not shown).

***sst2* Transfection Results in Both Decreased Bcl-2 Protein Expression and Stimulation of Mitochondrial Cytochrome c Release into the Cytosol.** Apoptosis mediated through the cell-intrinsic pathway involves activation or inhibition of proapoptotic and antiapoptotic Bcl-2 family genes (12). To investigate whether *sst2*-induced apoptosis depends on these proteins, we first analyzed Bcl-2 protein expression by Western blotting (Fig. 6a). *sst2* did not affect antiapoptotic Mcl-1, Bcl-X_L, and proapoptotic Bax or Bak protein expression levels (not shown), but antiapoptotic Bcl-2 protein expression was decreased (to $36 \pm 11\%$ of BxPC-3/mock cells) in BxPC-3/*sst2* cells ($P < 0.01$).

We then quantified cytosolic cytochrome *c* expression of mock- and *sst2*-transfected BxPC-3 cells (Fig. 6b). Using two separate anti-cytochrome *c* antibodies to first immunoprecipitate cytochrome *c* from cytosol cell fractions, and then to immunoblot cytochrome *c* in an SDS/PAGE gel, we demonstrated that cytochrome *c* was released into the cytosol of *sst2*-, but not of mock-transfected BxPC-3 cells (Fig. 6b Top). As a control for cytosolic crosscontamination by the mitochondrial fraction, we examined COXII expression in those cell fractions by Western blotting. As expected, COXII was expressed in the mitochondria, but not in the cytosol, of BxPC-3 cells (Fig. 6b Middle). These results suggest that *sst2*-induced apoptosis and cell-sensitization to death ligand-induced apoptosis might occur, at least in part, through an *sst2*-dependent activation of the cell-intrinsic pathway. To test this hypothesis, we investigated whether treatment of cells with HA14-1, a specific Bcl-2 inhib-

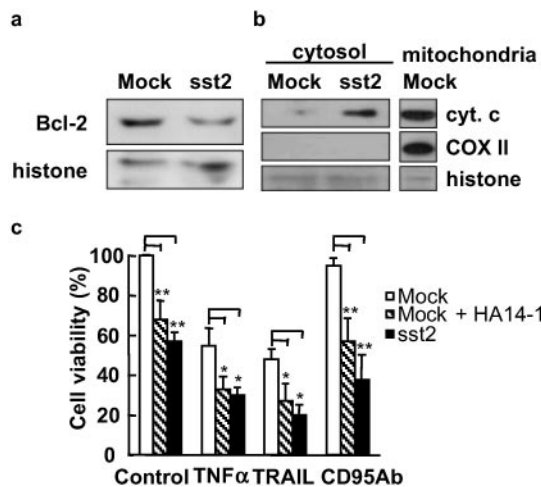


Fig. 6. Effect of sst2 transfection on mitochondrial Bcl-2 expression and cytochrome c localization in BxPC-3 cells. (a and b) Mock- and sst2-transfected BxPC-3 cells were grown (10^5 cells per ml) and starved for 24 h. (a) For immunoblotting, an anti-Bcl-2 antibody was used, and histone expression was utilized as an internal loading control ($n = 3$). (b) An immunoblot of cytosolic cytochrome c and histone expression in cytosolic extracts was used as an internal loading control. Expression of COXII was used as a cytosolic extract purity control ($n = 3$). (c) MTT assay. Mock- and sst2-transfected BxPC-3 cells were grown (10^4 cells per well) and treated for 24 h with TNF α + cycloheximide, TRAIL, or anti-CD95 Ab. Untreated cells were used as controls. Mock-transfected BxPC-3 cells were also treated (mock + HA14-1) or not treated (mock) with 50 μ M Bcl-2 inhibitor HA14-1. Data points represent the mean \pm SEM ($n = 4$) and are expressed as the percentage of cell viability observed in untreated mock-transfected cells (control mock). *, $P < 0.05$; **, $P < 0.01$ for HA14-1-treated mock-transfected cells and sst2- vs. mock-transfected cells.

itor, affects cell death in BxPC-3/mock cells and is able to mimic sst2-induced apoptosis. In the absence of cell stimulation by death ligand (control), pretreatment of cells with 50 μ M HA14-1 reduced the viability of BxPC-3/mock cells (to $68 \pm 9.5\%$ of control; $P < 0.01$), a level of cell viability measured in the untreated BxPC-3/sst2 cells ($57 \pm 4.7\%$; Fig. 6c). After cell treatment for 24 h with death ligands TNF α and TRAIL, the viability of BxPC-3/mock cells was decreased to $55 \pm 8.6\%$ and $48 \pm 5.2\%$, respectively, as compared with BxPC-3/mock cells not treated with death ligands, whereas CD95 Ab had only a minor effect (a 5% reduction). Strikingly, cotreatment of death ligand-stimulated BxPC-3/mock cells with HA14-1 affected the cell viability, reducing it to $33 \pm 6.5\%$, $P < 0.05$ for TNF α ; to $27 \pm 8.8\%$, $P < 0.01$ for TRAIL; and to $57 \pm 11.6\%$, $P < 0.01$ for CD95 Ab, as compared with the respective untreated cells. These levels of cell viability were similar to those measured in HA14-1-untreated death ligand-stimulated BxPC-3/sst2 cells ($30 \pm 4.1\%$ for TNF α , $20 \pm 5.4\%$ for TRAIL, and $38 \pm 12.4\%$ for CD95 Ab). We therefore concluded that the inhibition of Bcl-2 by HA14-1 in BxPC-3/mock cells mimics the sst2-induced decreased viability observed in BxPC-3/sst2 cells.

Discussion

Several lines of evidence indicate that sst2 behaves as a tumor suppressor for pancreatic cancer cells. Thus, we have previously demonstrated that stable sst2 gene transfection in pancreatic cancer cell lines, which do not endogenously express sst2, inhibits cell proliferation and tumorigenicity both *in vitro* and *in vivo*, and induces apoptosis *in vivo* (7, 8). The tumor suppressor effects of sst2 are based on a sst2-activated autocrine loop, because transfection of sst2 in cells lacking this receptor induces expression of its own ligand, somatostatin, which also constitutively activates sst2 (7, 9). Signal pathways implicated in apoptotic

effects of sst2 were investigated in sst2 gene-transfected polyclonal cells possessing an intact sst2-somatostatin autocrine loop, i.e., human pancreatic cancer BxPC-3 (BxPC-3/sst2) (7). Apoptosis was quantified and shown to be induced by sst2 in BxPC-3/sst2 cells. Interestingly, similar levels of apoptosis were observed in the present study by using an *in vitro* BxPC-3/sst2 model and in sst2-containing tumors generated from a s.c. injection of BxPC-2/sst2 cells to athymic mice (8). Previous studies have shown somatostatin-mediated induction of apoptosis in several cell models (17). Somatostatin receptor subtype 3 (sst3) was reported to be selectively involved in the somatostatin-induced apoptosis in CHO-K1 clones transfected with each of the five sst subtypes (18).

Strikingly, sst2 potently sensitized BxPC-3 cells to apoptosis induced by TNF α , TRAIL, or CD95 Ab, whereas these death ligands, except for TNF α in the presence of cycloheximide, did not efficiently stimulate apoptosis in mock-transfected cells. Quantification of cell viability by MTT assay, which was used as an alternative test to measure cell death, confirmed sst2-induced apoptosis and cell sensitization to death ligand-stimulated apoptosis. Because the specific executioner caspase inhibitor, DEVD-CHO, inhibited both sst2-induced apoptosis and sst2-mediated cell-sensitization to death ligand-induced apoptosis (not shown), we concluded that these sst2 effects were dependent on executioner caspases. This finding was confirmed by anti-caspase 3 and anti-PARP immunoblots, which showed cleavage of both the caspase 3 p11 subunit and PARP only in the death ligand-stimulated BxPC-3/sst2 cells, not in BxPC-3/mock cells. In addition, we demonstrated that sst2 sensitized BxPC-3 cells to death ligand-stimulated caspase 8, which indicates that the sst2-mediated cell sensitization to death ligand-induced apoptosis occurs, at least in part, at the level of the initiator caspase 8, upstream of the executioner caspases.

To identify the molecular mechanisms involved in sst2-induced apoptosis, we first demonstrated involvement of the SH2-containing tyrosine phosphatase SHP-1 in sst2-mediated cell death, because transfection of a catalytically inactive form of SHP-1 in BxPC-3 cells abrogated the proapoptotic action of sst2. We previously demonstrated that SHP-1 is a critical effector of sst2-mediated inhibition of cell proliferation and tumorigenicity (10, 16). SHP-1 has been also shown to be a critical component for induction of apoptosis by somatostatin in MCF-7 breast carcinoma cells, or by angiotensin II through the AT2 receptor (17, 19).

We then investigated the molecular mechanisms involved in sst2-mediated cell-sensitization to death ligand-induced apoptosis and executioner caspase activation.

First, we demonstrated that sst2 transfection in BxPC-3 cells induces expression of both the TNFR1 and DR4 proteins, at the posttranscriptional or transcriptional level, respectively, which indicates that sst2 might sensitize both cell lines to TNF α and TRAIL by increasing the number of their respective cell-surface receptors. This result also correlates with the sst2-dependent cell sensitization to death ligand-mediated activation of the initiator caspase 8. Transcriptional regulation of DR4 receptor expression has been documented in several epithelial cell models, and was shown to be induced after DNA damage through a p53-regulated pathway, or in a NF κ B-dependent manner (20, 21). In contrast, the regulation of TNFR1 has been poorly documented. Only one study reported the induction of TNFR1 mRNA expression by the inflammatory cytokine EMAP-II in human umbilical vein endothelial cells (22).

We then showed that sst2 sensitizes cells to death ligand-induced apoptosis by decreasing expression of the mitochondrial antiapoptotic protein, Bcl-2. sst2-dependent down-regulation of Bcl-2 expression was posttranscriptional, since no variation in the Bcl-2 mRNA was observed between BxPC-3/sst2 and BxPC-3/mock cells as assessed by real-time quantitative RT-PCR (not

shown). Translational regulation of the Bcl-2 protein by fibroblast growth factor-2 has been reported (23). HA14-1, a cell-permeable nonpeptidic ligand of Bcl-2, was shown to specifically inhibit biological function of Bcl-2 (24). We also demonstrate that suppression of Bcl-2 expression, resulting from treating the BxPC-3/mock cells with HA14-1, mimics sst2-inhibited viability of BxPC-3/sst2 cells. This finding strongly suggests that decreased Bcl-2 protein expression caused by sst2 might be involved in sst2-induced apoptosis and cell sensitization to death ligand-induced apoptosis. In addition, we proved that mitochondrial cytochrome *c* protein is released into the cytosol of BxPC-3/sst2, but not that of BxPC-3/mock cells, further confirming involvement of the cell-intrinsic mitochondrial pathway in sst2-induced apoptosis.

Dysregulation of the expression of several Bcl-2 family protein members, including Bcl-2, Bax, Bcl_{X_L}, or Mcl-1, has been demonstrated in human pancreatic adenocarcinoma (25), and shown to protect the pancreatic cancer cells from apoptosis induced by death ligands or chemotherapeutic drugs. In addition, in several pancreatic cancer cell lines, the Bcl-2 content is positively correlated, and the Bax/Bcl-2 ratio is negatively correlated with resistance of these cells toward chemotherapy or radiotherapy (25).

Pancreatic adenocarcinomas develop tumor escape mechanisms as a result of a dysregulation of the signaling pathways

involved in apoptosis mediated by death ligands and genotoxin drugs, which render this malignancy highly resistant to chemotherapy or radiotherapy (2), and also allow cancer cells to evade the immune surveillance (26), and consequently contribute to its rapid fatal course. Our work demonstrates that reexpression of a G protein-coupled receptor, sst2, in BxPC-3 human pancreatic cancer cells, which do not express endogenous sst2, not only induces cell death by apoptosis but also sensitizes these death ligand-resistant cells to apoptosis stimulated by TNF α , TRAIL, and FasL. Several studies have demonstrated that TRAIL can act as a potent anticancer agent, while causing no significant toxicity to normal tissues (27). These results, together with our findings that demonstrate marked sst2-mediated sensitization of the chemoresistant BxPC-3 cells to TRAIL-induced apoptosis, are of critical interest because combined gene therapy using both sst2 and TRAIL genes might lead to a novel approach to the treatment of human pancreatic adenocarcinoma.

We are grateful to C. Nahmias (Institut Cochin de Génétique Moléculaire, Paris) for providing SHP-1 constructs. This work was supported by Association pour la Recherche Contre le Cancer Grant 5576, Conseil Régional Midi-Pyrénées Grant 2ACFH0113C, Ligue Nationale Contre le Cancer Grant 2578DB06D, and European Community Contract QL3-CT-1999-00908.

1. Friess, H., Kleeff, J., Korc, M. & Buchler, M. W. (1999) *Dig. Surg.* **16**, 281–290.
2. Shi, X., Liu, S., Kleeff, J., Friess, H. & Buchler, M. W. (2002) *Oncology (Basel)* **62**, 354–362.
3. Schally, A. V., Comaru-Schally, A. M., Nagy, A., Kovacs, M., Szepeshazi, K., Plonowski, A., Varga, J. L. & Halmos, G. (2001) *Front. Neuroendocrinol.* **22**, 248–291.
4. Szepeshazi, K., Schally, A. V., Halmos, G., Armatos, P., Hebert, F., Sun, B., Feil, A., Kiaris, H. & Nagy, A. (2002) *Cancer Res.* **62**, 781–788.
5. Bousquet, C., Puente, E., Buscail, L., Vaysse, N. & Susini, C. (2001) *Chemotherapy* **47**, 30–39.
6. Buscail, L., Saint-Laurent, N., Chastre, E., Vaillant, J. C., Gespach, C., Capella, G., Kalthoff, H., Lluís, F., Vaysse, N. & Susini, C. (1996) *Cancer Res.* **56**, 1823–1827.
7. Delesque, N., Buscail, L., Esteve, J. P., Saint-Laurent, N., Muller, C., Weckbecker, G., Bruns, C., Vaysse, N. & Susini, C. (1997) *Cancer Res.* **57**, 956–962.
8. Rochaix, P., Delesque, N., Esteve, J. P., Saint-Laurent, N., Voight, J. J., Vaysse, N., Susini, C. & Buscail, L. (1999) *Hum. Gene Ther.* **10**, 995–1008.
9. Raully, I., Saint-Laurent, N., Delesque, N., Buscail, L., Esteve, J. P., Vaysse, N. & Susini, C. (1996) *J. Clin. Invest.* **97**, 1874–1883.
10. Benali, N., Cordelier, P., Calise, D., Pages, P., Rochaix, P., Nagy, A., Esteve, J. P., Pour, P. M., Schally, A. V., Vaysse, N., et al. (2000) *Proc. Natl. Acad. Sci. USA* **97**, 9180–9185.
11. Igney, F. H. & Krammer, P. H. (2002) *Nat. Rev. Cancer* **2**, 277–288.
12. Zimmermann, K. C., Bonzon, C. & Green, D. R. (2001) *Pharmacol. Ther.* **92**, 57–70.
13. Ibrahim, S. M., Ringel, J., Schmidt, C., Ringel, B., Muller, P., Koczan, D., Thiesen, H. J. & Lohr, M. (2001) *Pancreas* **23**, 72–79.
14. Cu villier, O. & Levade, T. (2001) *Blood* **98**, 2828–2836.
15. Sun, X. M., MacFarlane, M., Zhuang, J., Wolf, B. B., Green, D. R. & Cohen, G. M. (1999) *J. Biol. Chem.* **274**, 5053–5060.
16. Bousquet, C., Delesque, N., Lopez, F., Saint-Laurent, N., Esteve, J. P., Bedecs, K., Buscail, L., Vaysse, N. & Susini, C. (1998) *J. Biol. Chem.* **273**, 7099–7106.
17. Liu, D., Martino, G., Thangaraju, M., Sharma, M., Halwani, F., Shen, S. H., Patel, Y. C. & Srikant, C. B. (2000) *J. Biol. Chem.* **275**, 9244–9250.
18. Sharma, K., Patel, Y. C. & Srikant, C. B. (1996) *Mol. Endocrinol.* **10**, 1688–1696.
19. Cui, T., Nakagami, H., Iwai, M., Takeda, Y., Shiuchi, T., Daviet, L., Nahmias, C. & Horiuchi, M. (2001) *Cardiovasc. Res.* **49**, 863–871.
20. Guan, B., Yue, P., Clayman, G. L. & Sun, S. Y. (2001) *J. Cell. Physiol.* **188**, 98–105.
21. Ravi, R., Bedi, G. C., Engstrom, L. W., Zeng, Q., Mookerjee, B., Gelinas, C., Fuchs, E. J. & Bedi, A. (2001) *Nat. Cell Biol.* **3**, 409–416.
22. Berger, A. C., Alexander, H. R., Wu, P. C., Tang, G., Gnant, M. F., Mixon, A., Turner, E. S. & Libutti, S. K. (2000) *Cytokine* **12**, 992–1000.
23. Pardo, O. E., Arcaro, A., Salerno, G., Raguz, S., Downward, J. & Seckl, M. J. (2002) *J. Biol. Chem.* **277**, 12040–12046.
24. Wang, J. L., Liu, D., Zhang, Z. J., Shan, S., Han, X., Srinivasula, S. M., Croce, C. M., Alnemri, E. S. & Huang, Z. (2000) *Proc. Natl. Acad. Sci. USA* **97**, 7124–7129.
25. Miyamoto, Y., Hosotani, R., Wada, M., Lee, J. U., Koshiba, T., Fujimoto, K., Tsuji, S., Nakajima, S., Doi, R., Kato, M., et al. (1999) *Oncology* **56**, 73–82.
26. Elnemr, A., Ohta, T., Yachie, A., Kayahara, M., Kitagawa, H., Ninomiya, I., Fushida, S., Fujimura, T., Nishimura, G., Shimizu, K. & Miwa, K. (2001) *Int. J. Oncol.* **18**, 33–39.
27. Kagawa, S., He, C., Gu, J., Koch, P., Rha, S. J., Roth, J. A., Curley, S. A., Stephens, L. C. & Fang, B. (2001) *Cancer Res.* **61**, 3330–3338.